

PREDICTIVE CAPABILITY OF CONSTITUTIVE MODEL OUTSIDE THE RANGE OF CALIBRATION - COMPLAS XI

DAN WEDBERG^{*}, LARS-ERIK LINDGREN[†]

^{*} AB Sandvik Coromant, Metal Cutting Research, 811 81 Sandviken, Sweden
e-mail: dan.wedberg@sandvik.com, www.sandvik.com

[†] Division of Material Mechanics
Luleå University of Technology, SE-971 87 Luleå, Sweden
email: lars-erik-lindgren@ltu.se, www.ltu.se

Key words: Machining, Material model, Dislocation density, Extrapolation, High strain rates.

Abstract. Machining one of the most common manufacturing processes within the industry but it is also a process with extreme conditions in the vicinity of the cutting insert. Due to diversity of physical phenomena involved machining has proven to be complex and difficult to simulate. The chip formation process is in the vicinity of the cutting insert associated with highly localized severe deformations accompanied by high local temperatures rise. Furthermore, the strain rate can in the primary zone be very high ($>50000 \text{ s}^{-1}$), far beyond what can be reached with conventional mechanical material tests. Therefore, the possibility to extrapolate the material model outside the calibration range with respect to strain rate is a wanted feature. It is recognized that the mechanical behavior at high strain rate differs considerably from that observed at low strain rates and that the flow stress increase rapidly with the strain rates above $\sim 1000 \text{ s}^{-1}$. The predictive abilities outside as well as inside the calibration range of the empirical Johnson-Cook plasticity model and a dislocation density based model are compared and discussed with reference to AISI 316L stainless steel. The results clearly show the difficulty of obtaining a comprehensive material model that predicts the material behavior across the loading conditions that can occur in machining with good accuracy and that the accuracy of extrapolation is uncertain.

1 INTRODUCTION

Machining is a well recognized manufacturing process and one of the most common within the industry. Understanding of the material removal process is highly important and the ability to simulate machining are several, including determination and optimization of cutting tools design, cutting parameters, residual stresses and cutting process robustness to name a few. Machining has however proven to be particularly complex to simulate due to several numerical as well as modelling complications [1]. The work piece material during machining is forced to quickly change flow direction at the cutting edge vicinity to subsequently form a chip. These prerequisite give mainly rise to two main deformation zones, which are usually called the primary and the secondary deformation zone [1]. A third deformation zone can also be identified opposite the flank of the insert [2]. The major shearing of the work piece material takes place in the primary deformation zone and in addition to severe plastic

deformation and dissipated heat generations the strain rate can reach $> 50000 \text{ s}^{-1}$ within this zone [3]. The secondary deformation zone occurs in the contact between the chip and the insert after the material has gone through the first deformation zone. Due to the severe contact conditions with sticking and sliding at high pressure the local temperature is high within this zone. Heat is generated due to plastic generation and friction. Hence during machining the workpiece material locally experience severe strains, high strain rates and high temperatures causing hardening and softening. A material model must handle the involved complex interactions phenomena as plasticity, friction, heat generation, heat flow, material damage and microstructural changes of the workpiece material in order to be able to handle a wide range of strains, strain rates and temperatures.

The calibration of any material model is usually done based on data from material testing covering the relevant range of loading conditions of the intended application. The magnitude of strains, strain rate and temperatures involved in machining are however several orders higher than can be generated from conventional material tension and compression testing. Despite the fact that Split-Hopkinson is a technology that is becoming more common and that a strain rate of 10000 s^{-1} with large plastic strains [4] can be reached it is not sufficient to reach the extreme conditions that arise in the area around the cutting insert. Therefore the possibility to extrapolate the material model outside the calibration range without loss of accuracy is a highly wanted feature. This is not entirely trivial since materials exhibit different strain hardening and softening characteristic at different strain, strain rate and temperatures and that a marked increase in the strain rate sensitivity has been noticed for strain rates higher than approximately 1000 s^{-1} [5,6]. This significant increased strain rate sensitivity has been interpreted to different mechanisms for example increased dominance of dislocation drag [5], enhanced rate of dislocation and twin generation [6].

Considerable amount of work has been devoted to develop material models. The models can be divided into two major categories, empirical material models and physically based material models. The empirical models are solely based on curve fitting without any interpretation of the underlying physics and the deformation mechanisms. Hence the need for material data is relatively small which together with few parameters making them easy to use. The Johnson-Cook, J-C, plasticity model is an empirical material model that has been widely used to characterize the material response and is commonly used in FE-simulation of metal cutting. The physical based material models are on the other hand related to the underlying physics of deformation and the evolution of the microstructure. The predictive capabilities beyond the calibration range are therefore expected to be larger and more suitable for simulation of manufacturing processes involving large range and severe conditions of deformation, deformation rate and temperature. The predictive abilities outside as well as inside the calibration range of the empirical J-C plasticity model and a dislocation density based model, physical based, are in this study compared and discussed with reference to 316L stainless steel.

2 MATERIAL MODELS

2.1 Johnson-Cook plasticity model

The flow stress response of the J-C plasticity model is a multiplication of the individual strain, strain rate and temperature effects and is written

$$\sigma_y = \left(A + B \bar{\epsilon}^{p^n} \right) \left[1 + C \ln \left(\frac{\dot{\bar{\epsilon}}^p}{\dot{\bar{\epsilon}}_{ref}} \right) \right] \left[1 - \left(\frac{T - T_{room}}{T_{melt} - T_{room}} \right)^m \right] \quad (1)$$

where $\bar{\epsilon}^p$ is the effective plastic strain, $\dot{\bar{\epsilon}}^p$ is the effective plastic strain rate, $\bar{\epsilon}_{ref}$ represents a reference strain rate, T_{melt} is the melting temperatures, T_{room} is the room temperature. Parameters A , B , C , n and m are fitted user defined material parameters.

2.2 Dislocation density model

Dislocations and their motions have a decisive role in inelastic deformation of metals and alloys, especially at room temperatures. Their motion through the crystals of a polycrystalline material and their interaction is however a complex phenomenon. The model presented here assumes that dislocation glide is the dominant contribution to plastic straining. Climb is also included. The dislocation density model includes a coupled set of evolution equation for the state variables, dislocation density and vacancy concentration, in order to keep track of the hardening/softening behavior of the material [7,8,9].

The macroscopic flow stress is assumed to consists of additive components as in this case consists of three components according to

$$\sigma_y = \sigma_G + \sigma^* + \sigma_{drag} \quad (2)$$

where σ_G and σ^* are the long-range athermal component respectively the short-range contributions to the flow stress. The last component, σ_{drag} , accounts for phonon and electron drag. The first component, σ_G , is the stress needed to overcome the long-range interactions lattice distortions due to the dislocation substructure and grain boundaries. The second component, σ^* , is the stress needed for the dislocation to pass through the lattice and to pass short-range obstacles. Thermal vibrations will then also assist the dislocation when passing these obstacles. The long-range stress component is commonly written as

$$\sigma_G = m \alpha G b \sqrt{\rho_i} \quad (3)$$

where m is the Taylor orientation factor, α is a proportionality factor, G is the temperature dependent shear modulus, b is the magnitude of Burgers vector and ρ_i is the immobile dislocation density.

The short-range stress components may be written as,

$$\sigma^* = \tau_0 G \left(1 - \left(\frac{kT}{\Delta f_0 G b^3} \ln \left(\frac{\dot{\bar{\epsilon}}_{ref}}{\dot{\bar{\epsilon}}^p} \right) \right)^{1/q} \right)^{1/p} \quad (4)$$

where Δf_0 denote the required free energy needed to overcome the lattice resistance or obstacles without assistance from external stress, τ_0 denote the athermal flow strength required to move the dislocation past barriers without assistance of thermal energy,

$\dot{\bar{\epsilon}}_{ref}$ denote the reference strain rate. The exponent p and q characterize the barrier profiles and usually have values between $0 \leq p \leq 1$ respectively $1 \leq q \leq 2$.

The component that accounts for phonon and electron drag is written as [8]

$$\sigma_{drag} = G \left(C_e + C_p \frac{T}{300} \right) \dot{\bar{\epsilon}}^p \quad (5)$$

where T denotes the temperature, G the shear modulus, C_e and C_p is the electron drag respectively the phonon drag coefficient.

The evolution of the structure is considered to consist of a hardening and a recovery process. The total dislocation density may be characterized by the creation process, the immobilization process where dislocation get stucked, the re-mobilization process where the opposite occur and the annihilation process [7]. The total dislocation density in this model is considered to consist of both immobile dislocation density and mobile dislocation density. The used model assumes that the mobile dislocation density is stress and strain independent and much smaller than the immobile ones. Hence the evolution equation is written

$$\dot{\rho}_i = \dot{\rho}_i^{(+)} - \dot{\rho}_i^{(-)} \quad (6)$$

where index i denotes the immobile dislocations. It has been observed that dislocation tends to cluster into cells and subgrains during plastic deformation [10] and forming LEDS (Low-Energy Dislocation Structures) [11]. This structure evolution influences both the hardening and the recovery. The increase in immobile dislocation density is assumed to be related to the plastic strain rate and may therefore be written according to

$$\dot{\rho}_i^{(+)} = \frac{m}{b} \frac{1}{\Lambda} \dot{\bar{\epsilon}}^p \quad (7)$$

where Λ denote the mean free path which is a function of the size of the grains and the dislocation subcell diameter. The mean free path is assumed to be a combination of the distance between the grain boundaries, g , and the dislocation subcell diameter, s , as

$$\frac{1}{\Lambda} = \left(\frac{1}{g} + \frac{1}{s} \right) \quad (8)$$

where s is defined as

$$s = K_c \frac{1}{\sqrt{\rho_i}} + s_\infty \quad (9)$$

Reduction in dislocation densities may occur by different processes eg by dislocation glide and/or climb. This model takes into account the recovery by dislocation glide and climb. The former is described by

$$\dot{\rho}_i^{(-)} = \Omega \rho_i \dot{\bar{\epsilon}}^p \quad (10)$$

where Ω is a recovery function which may depends on the temperature and strain rate. Although in this model only of the temperatur. Recovery by climb is describe by

(11)

$$\dot{\rho}_i^{(-)} = 2c_\gamma D_v \frac{c_v}{c_v^{eq}} \frac{Gb^3}{kT} (\rho_i^2 - \rho_{eq}^2)$$

where c_v is the vacancy fraction, c_v^{eq} is the thermal equilibrium vacancy concentration, D_v is the diffusivity and c_γ is a calibration parameter. More details are found in [9].

2.3 Calibration procedure

The calibration of the presented dislocation density model and the J-C model was based upon uniaxial compression tests of SANMAC 316L at low strain rates, with a maximum strain rate and elevated temperature of 10 s^{-1} respectively $1300 \text{ }^\circ\text{C}$, and at high strain rates, with a maximum strain rate and elevated temperature of 9000 s^{-1} respectively $950 \text{ }^\circ\text{C}$. The temperatures were measured during the test at the low strain rates while computed assuming adiabatic heating for the tests at higher strain rates. The tests at the higher strain rates were performed via a Split-Hopkinson pressure bar (SHPB). The actual parameter determinations were done by an error minimization method via a developed toolbox in Matlab in combination with a subset of test data.

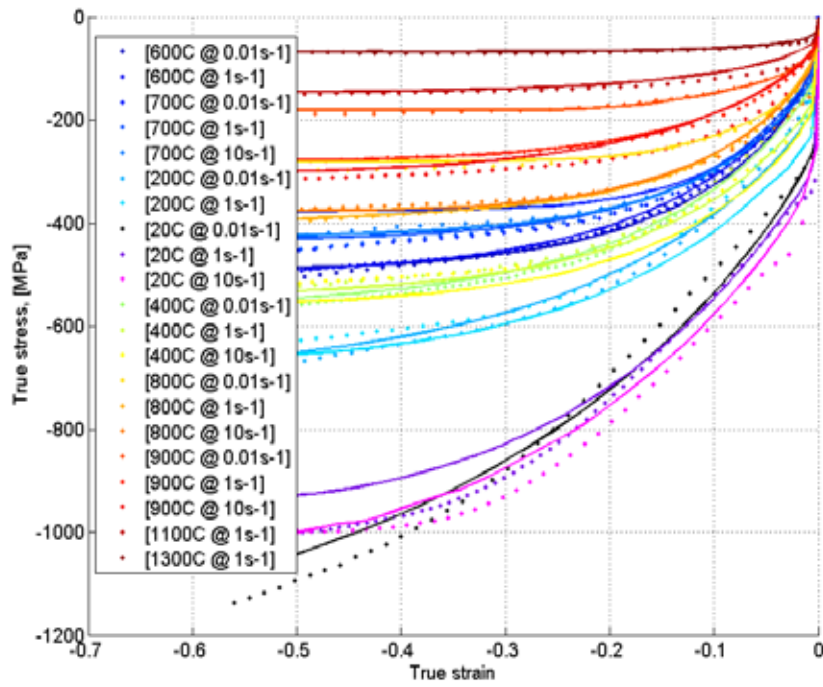
The parameters that need to be determined in the dislocation density model are shown in Table 1. Of these are the parameters K_c and Ω temperature dependent. A linear interpolation has been used between each test temperature and therefore each one of them has 9 values to be calibrated. Thermal expansion, Young's modulus, Poisson's ratio and shear modulus are also needed along with other physical constants. More details are given in [9]. The five parameters to be determined for the J-C model are given in section 2.1.

Table 1: Parameters to be determined in the dislocation density model

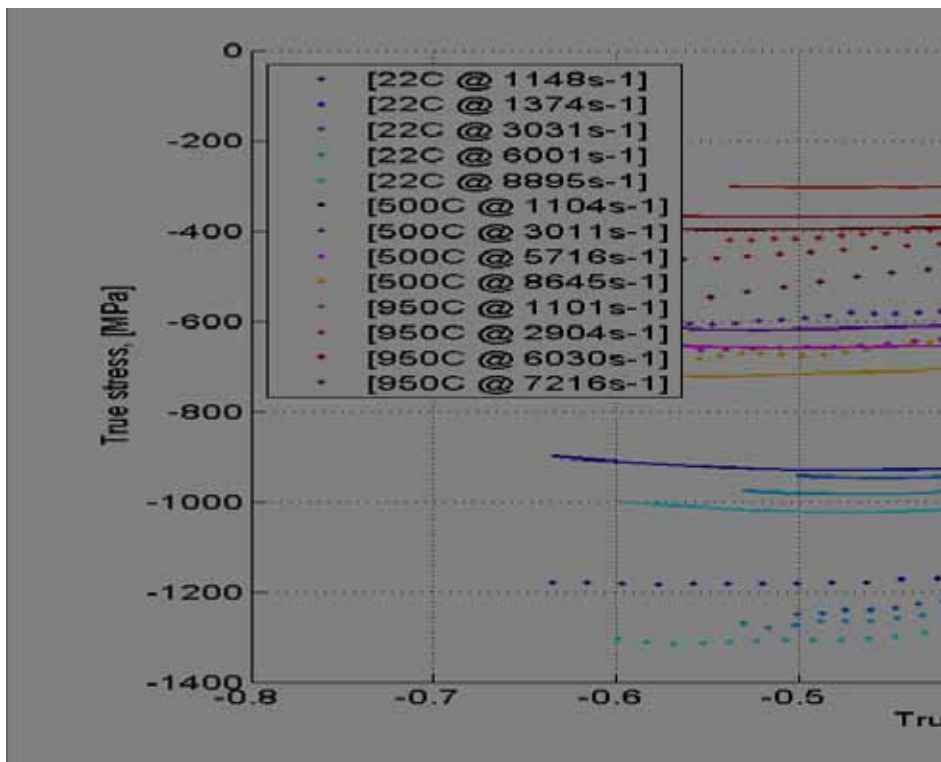
α	K_c	s_∞	ρ_{i0}	Ω	c_γ	τ_0	Δf_0	p	q	c_s^{Cr}	h^{Cr}	c_s^{Ni}	h^{Ni}	C_p	B_e/B_p
----------	-------	------------	-------------	----------	------------	----------	--------------	-----	-----	------------	----------	------------	----------	-------	-----------

3 RESULTS AND DISCUSSIONS

The dislocation density model has shown to give an overall good agreement with measured stress-strain curves in the strain rate range from 0.01 to 10 s^{-1} and from room temperature up to $1300 \text{ }^\circ\text{C}$ [9]. But if this material model with the optimized parameters at low strain rates are extrapolated and compared with measured stress-strain curves at high strain rates the same good agreement are not obtained. This was shown in [12]. Hence this discrepancy indicates that new physics are entering during deformation at these high strain rates and extrapolation from these conditions did not work. The observed increased strain rate sensitivity has been interpreted to different mechanisms for example increased dominance of dislocation drag [5], enhanced rate of dislocation and twin generation [6]. In an attempt to improve the predictability of the model throughout the strain rate range from low to high the physical phenomena dislocation drag has been implemented followed by a re-calibration of the model with given conditions. Some examples of measured stress-strain curves compared with predicted response of the dislocation density model at low strain rates and high strain rates are shown in Figure 1 at some different temperatures. The presented strain rate is the average strain rate.



a)



b)

Figure 1: Measured stress-strain curves and predicted response of the dislocation density model, lines, a) at low strain rates and b) high strain rates. Note: the vertical sequence of the curves fall with increased strain rate and reduced temperature.

The consistency at low strain rates is still good but the same consistency is not obtained at high strain rates. The predicted responses at 500 °C are little to high while little too low at room temperatures within the high strain rate range. Hence, dislocation drag followed by the re-calibration is not sufficient in order to cover the whole strain rate range from low to high. This indicates that additional and/or other deformation mechanisms are active and that the underlying dominated deformation mechanism changes. This will not be discussed further here. However, it is possible to get a relatively good consistency within the high strain rates range. Figure 2 shows the results from a re-calibration of K_c and Δf_0 based on data at high strain rates.

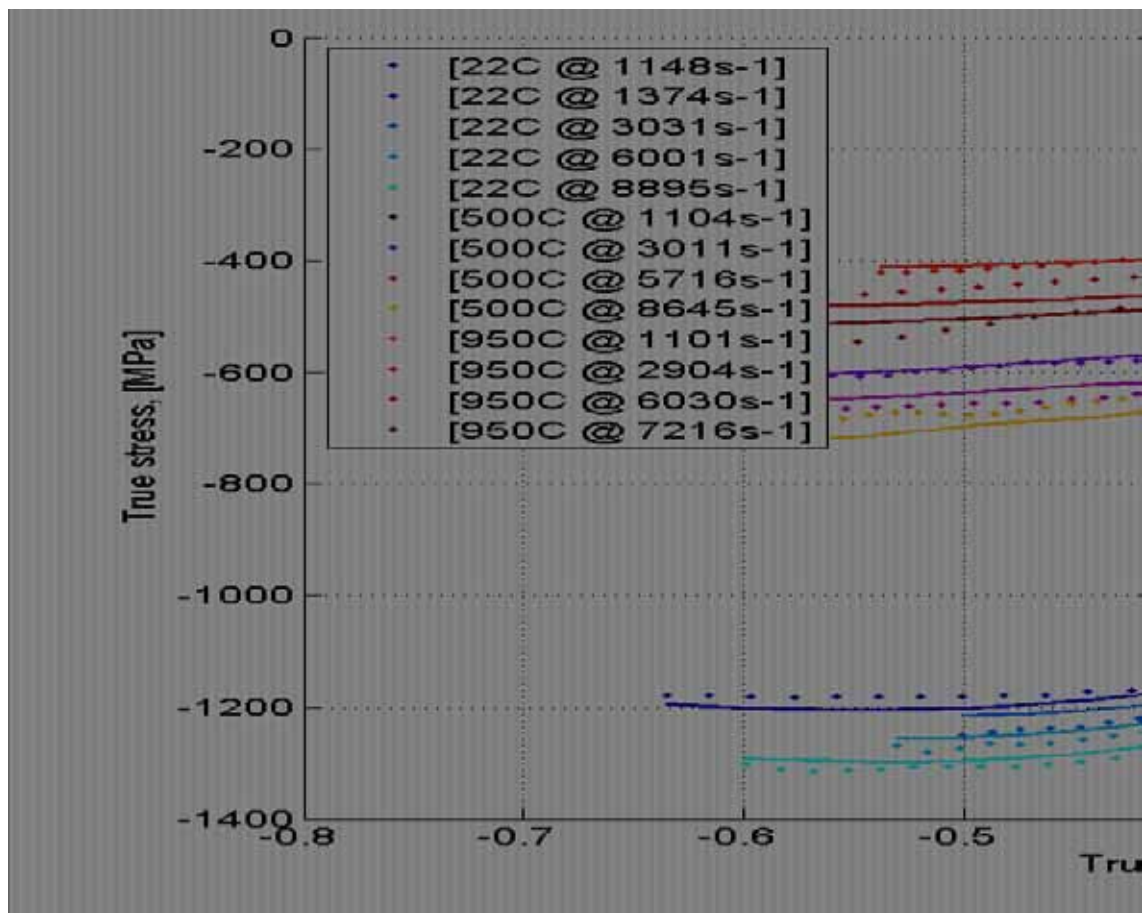


Figure 2: Measured stress-strain curves and predicted response of the dislocation density model, lines, where the latter is re-calibrated based on high strain rate data. Note: the vertical sequence of the curves fall with increased strain rate and reduced temperature.

The J-C plasticity model did not show the same consistency as the dislocation density model when subjected to the entire test data at low strain rate in [9] and it also failed to predict the material response at high strain rates with good agreements [12]. Better agreement, but far from satisfactory, was obtained if the parameters were re-calibrated based on only high strain data. The parameter and the predicted response are shown in Table 2 and Figure 3. The predicted responses at 950 °C and at room temperature are too low together with

significant differences in the work hardening rate at the latter temperature.

Table 2: Parameters for J-C plasticity model within the high strain rate range

Case	A	B	n	C	$\dot{\epsilon}_{ref}$	m
High	245 MPa	580 MPa	0.587	0.117	1 s^{-1}	0.733

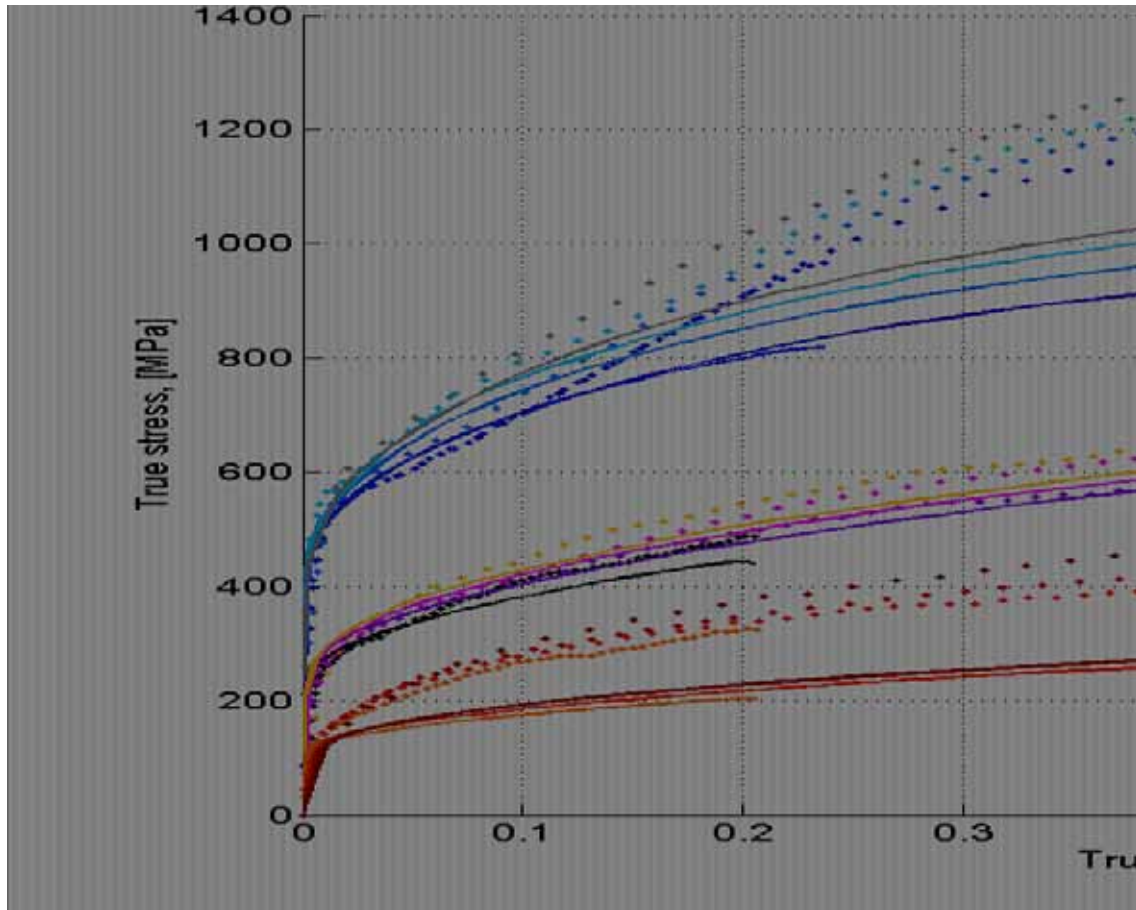


Figure 3: Measured stress-strain curves and predicted response of the J-C plasticity model, lines, where the latter has been re-calibrated based on high strain rate data. Note: the vertical sequence of the curves fall with reduced strain rate and increased temperature.

The reliability of extrapolation has so far proven to be uncertain. Although a wide available strain rate data range with a maximum strain rate of about 10000 s^{-1} extrapolation to even higher strain rates is needed to cover the loading conditions that may appear in machining simulations. Lack of material data at these extreme strain rates means that it is neither possible to calibrate or check the predictability range of the material model and it makes it even more uncertain. Despite this an extrapolation to strain rates up towards 50000 s^{-1} were performed based on the calibrated dislocation density model and the J-C plasticity model at high strain rates shown in Figure 2 and 3. The results are shown in Figure 4 together with presented results from SHPB-testing of 316L at a plastic strain of 0.1 and room temperature in

[12]. The difference in the predicted results between the dislocation density model and the J-C model, when extrapolated to these extreme strain rates, is noticeable. The predicted strain rate sensitivity is higher in the latter and has an appearance that complies with the current perception of increased strain rate sensitivity $> 1000 \text{ s}^{-1}$ but how precisely the extrapolation corresponds with the behavior of the material is difficult to say. More research is still needed.

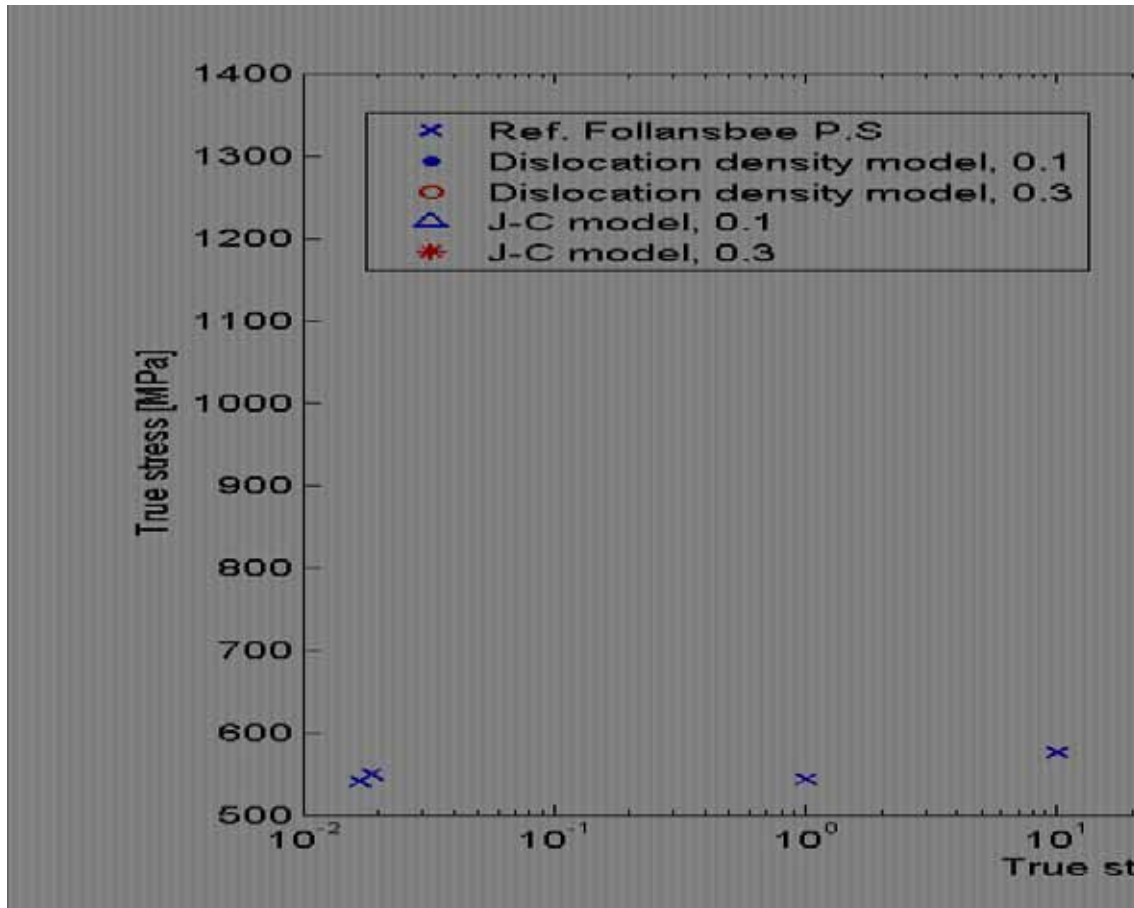


Figure 4: Measured flow stress, presented in [12], and predicted flow stress of the dislocation density model and the J-C plasticity model as function of strain rate at true strain of 0.10, 0.30 and room temperature. The dislocation density model and the J-C model are based on calibration at high strain rate data.

4 CONCLUSION

- The J-C plasticity model did not show the same good ability as the dislocation density model to reproduce the material behavior in the strain rate range and temperature range from 0.01 to 10 s^{-1} respectively from room temperature to $1300 \text{ }^\circ\text{C}$. Neither the dislocation density model without phonon drag nor the J-C model predicted the material behavior at high strain rates particularly well when extrapolated.
- Inclusion of phonon and electron drags within the dislocation density model improved the accuracy in the high strain rate range without any major changes in its prediction capability at low strain rates as the effects of phonon and electron drags

are small at these strain rates. The predictability is much better than the J-C plasticity model. However, we still consider the agreement with measurements to be somewhat unsatisfactorily. The discrepancy may be due to other deformation mechanisms or can be due to uncertainties and assumptions in the SHPB-testing.

- Extrapolated dislocation density model, calibrated with stress-strain data at high strain rates, shows higher strain rate sensitivity within the strain rate range of 10000-50000 s⁻¹ than the extrapolated J-C plasticity model calibrated within the same data range. This is due to the linear dependency on strain rate for the phonon-term whereas the J-C model has a logarithmic dependency. However, we have not data available to validate the predictable ability.
- The work clearly shows the difficulty of obtaining a comprehensive material model that predicts the material behavior across the loading conditions that can occur in machining with good accuracy.

ACKNOWLEDGEMENT

Swedish Research Council, grant no 1397-2005.

REFERENCES

- [1] Vaz, Jr., Owen, D., Kalhori, V., Lundblad, M., Lindgren, L-E. Modelling and simulation of machining processes. *Arch Comput Methods Eng* (2007) **14**:173-204.
- [2] Altintas, Y. *Manufacturing automation*. Cambridge University Press, (2000).
- [3] Poulachon, G., Moisan, A., Jawahir, I.S. On modelling the influence of thermo-mechanical behavior in chip formation during hard turning of 100Cr6 bearing steel. *Annals of CIRP* (2001) **50/1**:31-36.
- [4] ASM Handbook. *Mechanical testing and evaluation*. Vol. 8., (2000).
- [5] Regazzoni, G., Kocks, U.F., Follansbee, P.S. Dislocation kinetics at high strain rates. *Acta Metall* (1987) **35**:2865-2875.
- [6] Lee, W.S., Lin, C.F., Liu, T.J. Strain rate dependence of impact properties of sintered 316L stainless steel. *Journal of Nuclear Materials* (2006) **359**:247-257.
- [7] Bergström, Y. A dislocation model for the stress-strain behavior of polycrystalline α -Fe with special emphasis on the variation of the densities of mobile and immobile dislocations. *Materials Science & Engineering* (1969/70) **5**:193-200.
- [8] Frost, H.J., Ashby, M.F. *Deformation-Mechanism Maps – The Plasticity and Creep of Metals and Ceramics*. Pergamon Press.
- [9] Lindgren, L.-E., Domkin, K., Hansson, S. Dislocation, vacancies and solute diffusion in physical based plasticity model for AISI 316L. *Mech. of Materials* (2008) **40**:907-919.
- [10] Holt, D. Dislocation cell formation in metals. *Journal of Applied Physics* (1970) **41**(8):3197-3201.
- [11] Kuhlman-Wilsdorf, D. Q:Dislocation structure – how far from equilibrium? A: Very close indeed. *Materials Science & Engineering* (2001) **A315**:211-216.
- [12] Lindgren, L.-E., Wedberg, D. Material modelling and physical based models with particular emphasis on high strain rates, in: A, K. (Ed), *International Symposium on Plasticity* (2009). NEAT, Inc, St Thomas, USA.
- [13] Follansbee, P.S. High-strain-rate deformation of FCC metals and alloys, in

Metallurgical applications of shock-wave and high-strain-rate phenomena, Murr, L.E., Staudhammer K.P., Meyers, M.A. (Ed) (1986).